Journal of Imaging Science and Technology® 64(6): 060406-1–060406-7, 2020.

Exploring the Facial Color Representative Regions Using the Humanae Images

Yuchun Yan▲
Department of Industrial Design, KAIST, Daehak-ro 291, Yuseong-gu, Daejeon, South Korea

Hayan Choi
DeepScent, Daejeon, Korea

Hyeon-Jeong Suk
Department of Industrial Design, KAIST, Daehak-ro 291, Yuseong-gu, Daejeon, South Korea
E-mail: color@kaist.ac.kr

Abstract. *It is difficult to describe facial skin color through a solid color as it varies from region to region. In this article, the authors utilized image analysis to identify the facial color representative region. A total of 1052 female images from Humanae project were selected as a solid color was generated for each image as their representative skin colors by the photographer. Using the open CV-based libraries, such as EOS of Surrey Face Models and DeepFace, 3448 facial landmarks together with gender and race information were detected. For an illustrative and intuitive analysis, they then re-defined 27 visually important sub-regions to cluster the landmarks. The 27 sub-region colors for each image were finally derived and recorded in L*, a*, and b*. By estimating the color difference among representative color and 27 sub-regions, we discovered that sub-regions of below lips (low Labial) and central cheeks (upper Buccal) were the most representative regions across four major ethnicity groups. In future study, the methodology is expected to be applied for more image sources.* © *2020 Society for Imaging Science and Technology.*
[DOI: 10.2352/J.ImagingSci.Technol.2020.64.6.060406]

1. INTRODUCTION

Although human skin color varies within a relatively narrow range in color hue, our visual system has been evolved to be sensitive to distinguish the subtle differences. It is related to the notion of memory color that the human vision system pursues viewing the human skin color in a fixed value [1]. On this ground, studies on color correction have tried to detect the human skin in digital images by using human skin as the calibration target. For example, Bianco and et al. [2] achieved color constancy using the human face, and Xie and et al. [3] used the color of the human hand an alternative but practical target. More recently, Yan and Suk [4] examined different visual appeal varied by the articulated hue nuance of human skin.

Accordingly, many studies have tried to propose the true color of human skin, and various findings are meaningful. Not to mention the ethnicity or demography aspects, such as gender [5] or age [6], the medium facial images also affect our judgement whether the skin color is correctly reproduced or visualized within a perceptual tolerance. Some researchers claimed that we expect much lighter color when we recall the human skin in digital display than in a standard illuminant, such as D65 [7, 8]. In the study, averaged color values in the skin region have been used mostly to detect the human face's color.

Admitting that the human face is three-dimensional (3D), some studies have tried to figure out the color difference within a person. They claim that the color variability within one's face is noticeable. Some researchers measured the skin color of the forehead and cheek region of four ethnic groups and showed that forehead and cheek regions had a significant color difference across the four ethnic groups [9]. One study found out that African-Americans' facial color showed a bigger variability than other ethnic groups [10]. The study discovered that the lightness difference between the forehead and cheek was remarkably different across four groups. The largest difference was found for Thai and the smallest for Caucasians.

Consequently, some studies proposed methods that capture the representative color from facial images. By convention, a small area in the cheek is often used [11, 12]. As a more refined guide, Kikuchi and et al. [13] considered the perpendicular intersection of the corner of the eye and lip as the skin color representative region. Hsiao and et al. [14] referred an average of six points made up of four points in both cheeks, one in the chin, and one in the forehead. Choi, Choi and Suk [15] suggested an average of a rectangular region defined by the eye center and nose tip as the horizontal and vertical boundaries. Alternatively, Kikuchi and et al. [6] observed the entire cheek area admitting that a single spot may bias the capture of one's skin color. The diverse approaches are supported by different rationale, thereby remaining the color representative facial region equivocal.

In this study, we pay attention to the "Humanae" project created by Angélica Dass, which adopted the format of

▲ IS&T Member.

Received July 14, 2020; accepted for publication Nov. 13, 2020; published online Dec. 30, 2020. Associate Editor: Rita Hofmann-Sievert.
1062-3701/2020/64(6)/060406/7/$25.00

Figure 1. Some examples of the facial images from the Humanae project at www.angelicadass.com. We initially scraped 2231 images consisting of diverse demographic and ethnic profiles and later selected 1052 women faces, the facial landmark was properly fitted.

the PANTONE® Guide. It is a collection of over 2000 facial images that cover diversity in both ethnicity and demography. Some of the examples were shown in Figure 1. When the artist photographed a person, she customized the background color as the representative solid color for the person's facial color. Utilizing this image data set and the customized representative skin color for each image, we intended to discover a facial region that is illustrative enough to represent one's skin color. When that facial region is consistently applied to the majority of the images, we may conclude that we perceive one's facial color based on this specific region. We adopted open CV-based libraries to detect facial regions and identify both demographic and ethnic profiles for the analysis. Furthermore, we tried to utilize the method of dividing the human face into smaller sub-regions to draw perceptually meaningful conclusions.

1.1 *Facial Images: the "Humanae" by Angélica Dass*

We scrapped a total number of 2231 images from the "Humanae" project led by a photographer Angélica Dass (retrieved from https://www.angelicadass.com/). The project is a portrait data set consisting of volunteers without any limitation of nationality, gender, age, race, social class, or religion. In each facial image, the photographer deliberately tailored background color that should correspond to the person's representative color. Additionally, a code from the PANTONE® Guide is labeled underneath, that is, the nearest to the background color. The data set is a compelling resource to investigate the human skin color, and consequently, it has received considerable attention as a thoroughly documented and inspirational art project. The project participated in exhibitions internationally. Yet, only a few attempts were made to utilize the project as a precious resource for an imaging study. For example, researchers tried to associate geographical distribution based on one's skin tonality using the facial images downloaded from the Humanae project [16]. We were motivated to figure out the relationship between the facial images and the background in terms of color quantity. By examining the color difference between the background and regions within a face, we intended to identify a particular region that the artist considered facial color representative unconsciously. Supported by the open CV-based libraries and algorithms, such computational investigation easily results in quantitative evidence. Subsequently, the method we described in this study can be replicated with different image data sets.

2. METHOD

2.1 *About the Data set*

When we considered the link between facial region and color, the male adults with mustache and beard may mislead the correct match. Hence, we limited the women images only and acquired the gender classification of the scrapped images. We employed the DeepFace [17] library, the facial recognition algorithm developed by Facebook research group. Trained with four million images, its neural network is composed of

Table I. Gender and ethnicity classification of the 2231 facial images resulted from the DeepFace [17] library.

Races	Male	Female
Asian	97	76
Black	186	41
Indian	24	6
Latino Hispanic	145	103
Middle Eastern	61	10
White	665	817
Total	1178 (52.8%)	1053 (47.2%)

nine layers, and the accuracy is up to 97.35% reportedly. We adopted the algorithm for gender and ethnic classification to identify the dominant racial membership of each face, as presented in Table I. Caucasians occupy the majority labeled as "White" followed by "Latino Hispanic," "Black," "Asian," "Middle Eastern," and "Indian." As the images of the Humanae project have been built up based on volunteers, it has resulted in a uneven ethnicity distribution. Also, the gender proportion within each ethnicity group differs. Nonetheless, the overall gender ratio is balanced, having 52.8% for men and 47.2% for women.

2.2 *Mapping the Facial Landmarks to Face Sub-regions*

To identify sub-regions in each facial image, we initially adopted an OpenCV Face Recognition library, dlib [18]. The algorithm figures out the 68-point ibug annotations in each human face. The 68 points identify eyebrows, eyes, nose, mouth, and the contour of face reasonably well. The library has been broadly adopted in many recent studies on facial characteristics. However, for color analysis, we sub-divided the facial surface into smaller regions to correspond to the facial anatomy. Thus, to obtain more detailed landmarks within a face, we used the EOS library that applies the Surrey Face Model (SFM) [19] mesh vertex indices based on the 68 ibug annotations. The SFM mesh vertex included 845-point annotations, and the EOS library interpolated up to 3448-point annotations.

As the facial images in the Humanae project are looking forward, most of the images were well fitted to the landmark detection, as displayed in Figure 2 on the left. However, there were a few cases in that the mapped results are displaced like the right picture in Fig. 2. After screening all images mapped with SFM mesh, we filtered out four false mapping images from the analysis. The four images were made up of three men and one woman. As a result, the total number of 1052 women's facial images were taken to the analysis.

2.3 *Regional Units of Face*

To have a perceptually meaningful interpretation of the facial region and color, we tried to merge the mesh vertex with sub-regions in the perspective of facial anatomy. In sub-regions approaches, the face is divided into small but essential regions. There are several unique approaches to

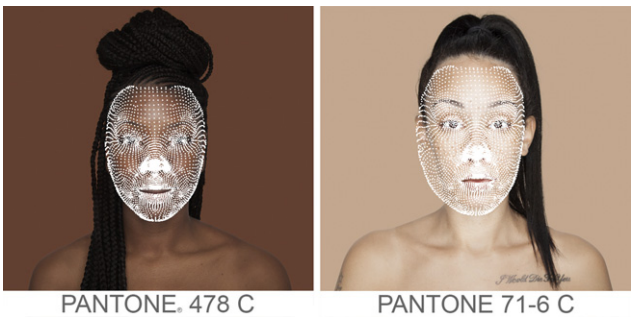

Figure 2. Overall, the 3448 vertices were well detected in faces, like the Pantone 478 C case (left). However, four images out of 2231 were exempt from the analysis because the dlib-based landmark detection was not successful (see the Pantone 71-6 C case on the right).

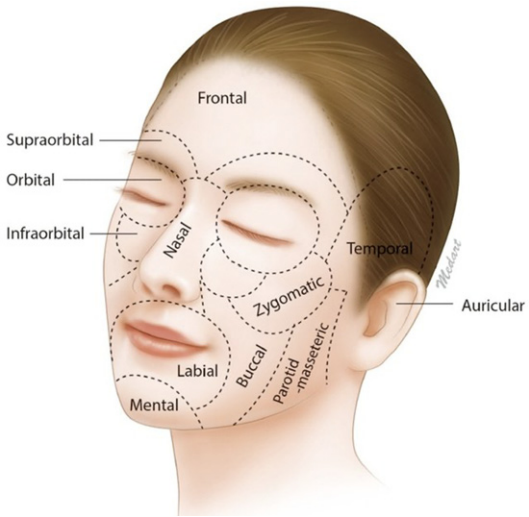

Figure 3. The facial aesthetic unit [21].

divide the facial regions into smaller areas depending on different concerns. For example, Poux and et al. [20] proposed a facial expression recognition algorithm in that the most relevant regions considering occlusions impacts. In the study, 25 regions were initially defined, that were laid out following the facial muscle scheme. In their study, the combinations of 25 regions were considered as the input of computation. However, we focused on sub-regions, where we can define visually distinct locations, rather than anatomical muscle structure or layer characteristics of the skin. Accordingly, we adopted the sub-region method proposed as a facial aesthetic unit [21] as illustrated in Figure 3. Having advanced the previous studies [21, 22] divided the face into 12 sub-regions. For example, they split the forehead into "frontal (central forehead)" and "temporal (forehead close to ears)" regions. Also, they divided the orbital region into three sub-regions, including "supraorbital (above the eyes)," "orbital (around the eyes)," and "infraorbital (underneath the eyes)." For defining the infraorbital region, the nasojugal fold was referred.

Regarding the five regions, including Frontal, Nasal, Zygomatic, Buccal, Parotid-masseteric, we considered adding sub-regions to detail the regions, because they

Table II. The 27 sub-regions matched to the aesthetic unit [21] and the corresponding locations.

Code	Aesthetic unit	Description	Horizontal location
f.c1	Frontal	Center of forehead	Center
f.c2	Frontal	Middle of eye brows	Center
f.l	Frontal	End of forehead	Left
f.r	Frontal	End of forehead	Right
n.c	Nasal	Nose bridge	Center
n.t	Nasal	Nose tip	Center
m	Mental	Chin	Center
l.r	Labial	Below lips	Right
l.l	Labial	Below lips	Left
s.r	Supraorbital	Above an eye	Right
s.l	Supraorbital	Above an eye	Left
o.r	Orbital	Low eye rim	Right
o.l	Orbital	Low eye rim	Left
i.r	Infraorbital	Below an eye	Right
i.l	Infraorbital	Below an eye	Left
z.r1	Zygomatic	Upper cheekbone	Right
z.r2	Zygomatic	Lower cheekbone	Right
z.l1	Zygomatic	Upper cheekbone	Left
z.l2	Zygomatic	Lower cheekbone	Left
b.r1	Buccal	Central cheek	Right
b.r2	Buccal	Lower cheek	Right
b.l1	Buccal	Central cheek	Left
b.l2	Buccal	Lower cheek	Left
p.r1	Parotid-masseteric	Upper jaw	Right
p.r2	Parotid-masseteric	Lower jaw	Right
p.l1	Parotid-masseteric	Upper jaw	Left
p.l2	Parotid-masseteric	Lower jaw	Left

included shadows within one region. For instance, we split the frontal region into four regions: center of the forehead, middle of eyebrows (i.e., "Glabella" region), left end of the forehead, and right end of the forehead. Both ends were near the temporal regions. On the contrary, the temporal regions were not taken because they were hardly visible from the forward-looking faces. Also, the Auricular regions were exempt since they were covered with hair. In this way, we finally completed a new set of facial sub-region that consists of 27 sub-regions. Detailed matching between 27 sub-regions and the aesthetic unit was listed in Table II and a comparison with the 3448 SFM vertices was presented in Figure 4.

2.4 *Vertex Matches with Facial Sub-regions*

To match the SFM vertices with the 27 sub-regions, we overlaid the wireframe of sub-regions of [21] shown in Fig. 4, on the selected facial images, chosen deliberately from one of each ethnicity group. For the selection, the criteria were whether the SFM mesh fit the facial image almost perfectly. We used the "Puppet Warp" command in Adobe® Photoshop® 2020 to fit the wireframes to the selected facial

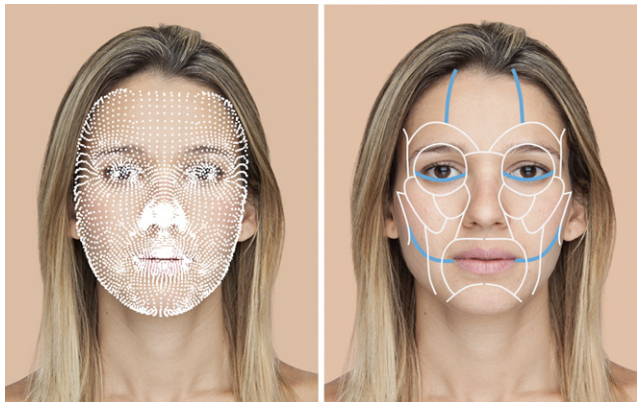

Figure 4. (Left) Pantone 57-6C was selected for sorting out the vertices into sub-regions. The 3448 SFM vertices are well fitted to the face. (Right) The face with 27 sub-regions. The sub-region was basically guided by the aesthetic unit proposed by Choi and et al. [21], and then more sub-regions were created in addition.

images manually for each of the selected six facial images. The command drags control points to manipulate the shape of sub-region wireframes to be fitted. After that, we picked vertices distributed in a central area of each sub-region. On average, 18.74 vertices were counted for each sub-region, and we obtained the corresponding pixel's RGB values. The vertex picking proceeded for the six selected facial images, and the judgements were based on the consensus among three researchers. In Figure 5, the three steps are illustrated in the case of an image labeled as Pantone 57-6C.

2.5 *Color Difference between the Target and Facial Sub-regions*

In Humanae's facial images, the artist defined the background color, considering it as the perceptually representative color of the facial skin. Thus, we tried to estimate the color difference between each sub-region and background, and then find out the sub-regions with the smallest color difference, ΔE. To compute the ΔE, we collected the RGB values of the pixels that corresponded to the vertex locations and then converted the RGB to $L^*a^*b^*$ values in CIE1976$L^*a^*b^*$ (CIELab). After the color conversion, we computed the ΔE, the Euclidean distance of two colors in CIELab color space. The ΔE is almost linearly mapped to the perception of color difference and employed in the analysis. Then we averaged the L^*, a^*, and b^* within each sub-region as well as the background. Declaring the background as a target color, an average L^*, a^*, and b^* of a sub-region$_{\text{frontal:left}}$ is defined as $L_{\text{frontal.left}}$, $a_{\text{frontal.left}}$, $b_{\text{frontal.left}}$. Consequently, the color difference between target and the sub-region (i.e., frontal.left) is measured as Equation 1 presents ($f.l$ = frontal.left). In this way, we estimated the color difference, ΔE with regard to the 27 sub-regions for the entire women faces.

$$\Delta E_{f.j} = \sqrt{(L^* - L^*_{f.l})^2 + (a^* - a^*_{f.l})^2 + (b^* - b^*_{f.l})^2} \quad (1)$$

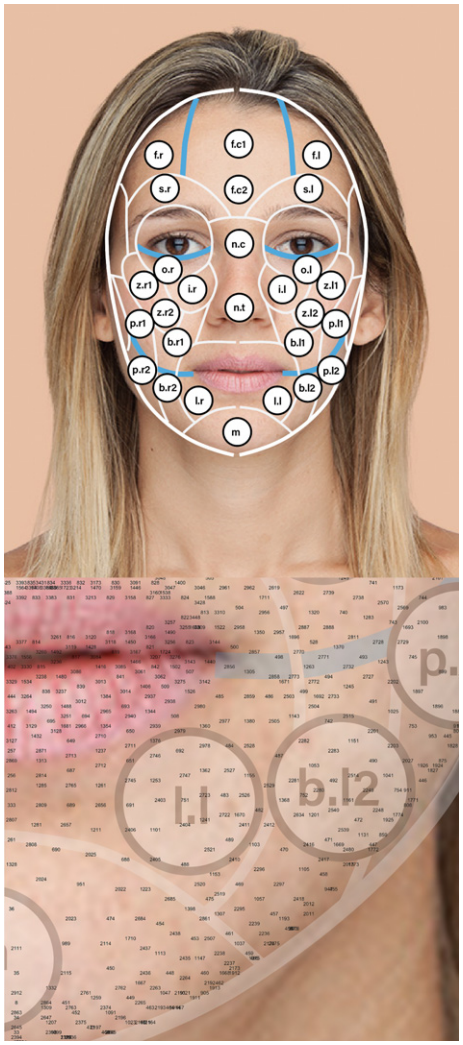

Figure 5. (Top) The color of 27 sub-regions were identified from the vertex locations within each circle. (Bottom) A zoom-in of lip area, where the SFM vertices and sub-regions are overlapped.

Table III. The average mean, standard deviation, and median values of color differences ΔE across the 27 sub-regions, indicating that color of both central cheek regions (b.l1 and b.r1) and below lip regions (l.l, l.r) are the closest to the target color. ($N = 1052$)

Rank	Code	Description	Mean (Standard deviation)	Median
1	l.l	Below lips	5.71(3.26)	5.05
2	b.l1	Central cheek	6.01(3.43)	5.26
3	b.r1	Central cheek	6.54(3.82)	5.71
4	z.r2	Lower cheekbone	7.24(4.28)	6.28
5	l.r	Below lips	7.24(4.10)	6.38
6	o.r	Low eye rim	7.63(4.67)	6.56
7	z.l2	Lower cheekbone	7.92(4.75)	6.90
8	n.c.	Nose bridge	8.35(5.35)	7.15
9	o.l	Low eye rim	8.69(5.14)	7.62
10	m	Chin	9.00(5.06)	8.00
11	z.l1	Upper cheekbone	9.06(8.27)	6.70
12	i.r	Below an eye	9.19(5.46)	8.06
13	z.r1	Upper cheekbone	9.74(8.57)	7.45
14	n.t.	Nose tip	9.80(6.06)	8.41
15	b.l2	Lower cheek	10.23(6.65)	8.76
16	i.l	Below an eye	10.55(5.94)	9.65
17	s.r	Above an eye	12.73(15.35)	6.97
18	f.c2	Middle of eye brows	13.39(8.56)	11.92
19	p.l1	Upper jaw	13.75(10.53)	11.10
20	s.l	Above an eye	14.07(15.90)	7.27
21	f.c1	Center in forehead	15.21(12.76)	11.34
22	b.r2	Lower cheek	19.10(12.13)	16.54
23	p.l2	Lower jaw	19.33(15.22)	14.96
24	p.r1	Upper jaw	20.42(12.12)	18.07
25	f.r	End of forehead	23.58(20.03)	15.21
26	p.r2	Lower jaw	25.05(16.45)	20.69
27	f.l	End of forehead	27.17(20.95)	20.16

3. RESULTS AND ANALYSIS

As we filtered women's faces from the entire image set, the analysis was applied to women only to avoid the color bias of mustache and beard in the case of men's faces. Excluding the false mapping result (shown in the right picture in Fig. 2), the facial images of 1052 women were used in the analysis. The images included 816 Caucasians followed by 103 Latino Hispanics and 76 Asians, as displayed in Table I. Based on the estimated color difference, we observed both the general tendency and ethnicity specific results.

First, to reveal the sub-region with a minimum color difference from the background target color, we estimated how the color difference increases across the entire 27 sub-regions. As shown in Table III, the color of upper Buccal and lower Labial regions is the closest to the target color followed by upper Zygomatic regions connected to the upper Buccal regions. In most previous studies on the skin color representative regions, spectrometers were facilitated as the apparatus to capture the reflectance of the target regions' visible wavelength range. For example, a perpendicular intersection of the corner of the eye and lip was chosen as the region [13]. However, when we face a person, the perpendicular intersection region appears in shadow because the human face is three-dimensional. Indeed the perpendicular intersection region corresponds to the Parotid-masseteric that are linked closely to "p.r1" and "p.l1" in this study. These regions are closest to the outer rim of the face when a person is looking forward. Accordingly, the perpendicular interaction region is darker than the "Buccal" and "Labial" regions.

Second, we tried to examine the color differences between sub-regions and background across the ethnicity groups. The DeepFace library figured out a total of six ethnicity groups labeled as "Asian," "Black," "Indian," "Latino Hispanic," "Middle Eastern," and "White" as presented in Table I. We excluded minority groups such as Indian and Middle Eastern among six ethnicity groups, as their sample sizes were 6 and 10, respectively. As shown in Table IV, in general, both areas below lips and central cheek were found to

Table IV. The average mean, standard deviation, and median values of color difference ΔE with top five closest sub-regions across four ethnicity groups.

Rank	Code	Description	Mean (Standard deviation)	Median
Ethnicity group: White ($N = 816$)				
1	l.l	Below lips	5.61(3.17)	5.00
2	b.l1	Central cheek	5.77(3.26)	5.05
3	b.r1	Central cheek	6.44(3.78)	5.59
4	z.r2	Lower cheekbone	6.49(3.49)	5.79
5	z.l2	Lower cheekbone	6.98(3.88)	6.19
Ethnicity group: Latino Hispanic ($N = 103$)				
1	l.l	Below lips	6.01(3.38)	5.31
2	l.r	Below lips	7.01(4.10)	6.09
3	b.r1	Central cheek	7.28(3.91)	6.88
4	b.l1	Central cheek	7.38(4.03)	6.67
5	z.l1	Lower cheekbone	8.90(6.65)	7.03
Ethnicity group: Asian ($N = 76$)				
1	l.l	Below lips	5.38(3.58)	4.41
2	b.l1	Central cheek	5.42(3.13)	4.76
3	b.r1	Central cheek	5.78(3.46)	5.16
4	l.r	Below lips	7.11(4.29)	6.22
5	o.r	Low eye rim	7.17(4.54)	5.95
Ethnicity group: Black ($N = 41$)				
1	l.r	Below lips	7.47(3.36)	6.77
2	l.l	Below lips	7.48(3.63)	6.86
3	b.r1	Central cheek	7.93(4.37)	7.00
4	z.r1	Upper cheekbone	8.23(4.98)	7.42
5	b.l1	Central cheek	8.32(3.90)	7.78

have the closest color to the background across the ethnicity groups. Among the four groups, "Black" shows a little bit bigger color difference; the order of sub-region still follows the general tendency though. Based on the computational findings, Figure 6 illustrates the four sub-regions, including central cheek and below lips on both left and right.

4. DISCUSSION

In this study, we explored the facial regions from that we perceptually judge one's face color. Having adopted a series of open CV-based libraries, we managed to derive a conclusion that color of upper Buccal (i.e., central cheek) and lower Labial (i.e., below lips) regions (shown in Fig. 6) can represent one's facial color.

When talking about the representative facial skin color, or representative facial skin region, each discipline pursues different values due to different concerns. For example, makeup artists might have their standards and understanding of it for base makeup color selection to make skin color even; practitioners in computer vision might have their method to extract this key solid color for image analysis. Based on their practical experience, it is also possible to discover the tendency.

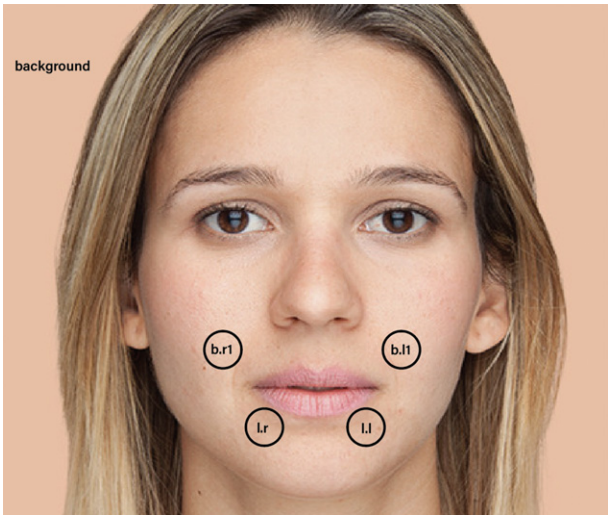

Figure 6. The color of central cheek and below lip regions were revealed to be the nearest to the background across ethnicity groups.

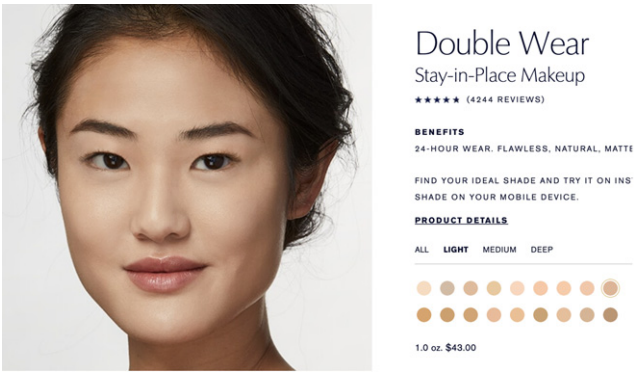

Figure 7. By convention, face makeup products are presented with a 2D color patch and a photographed facial image in that the product is being applied (www.esteelauder.com).

We tried a data-driven approach by having adopted some computational method to find the answer. As a result, we propose a new method that can be replicated with a different data set. Having combined existing algorithms and domain-specific knowledge, such as facial aesthetic unit from plastic surgery, we tried to establish a method for a particular purpose, finding facial color representative regions. To be specific, we used the well-established data libraries to detect facial landmarks, facial regions, gender, and ethnicity. Thus, the method is not limited to find the skin color representative regions. Any attempts related to the facial region with an emphasis on the aesthetic unit can adopt the method proposed in this study. For example, a color scheme or makeup style can be easily and quickly detectable. Also, color variability within one's face can be a possible related topic. As shown in Figure 7, consumers are informed about the facial cosmetic products by viewing both a two-dimensional (2D) color patch and an applied face thereof. Professional photographers make a great effort to match the perceptual colors between these two. Our method may contribute to the optimal understanding of the perceptual color match

between the 2D color patch and 3D photography in a future study.

However, this study's findings are limited to the assumption that the background color of Humanae's facial images is truly representative of the facial images that the general audience is likely to agree with. Understanding an artist's intention as such is valuable work, but it can also be arguable when we want to generalize our findings based on a particular artwork. Although the examination has been conveyed with more than 1000 images, the finding may vary depending on the images. Thus, further investigations are expected to verify the results and find additional observations between the facial region and the face's perceptually representative color.

Furthermore, in the making of facial sub-regions, a future study can consider different methods depending on the research concern. Led by studies on facial expression, several sub-region techniques have been introduced in face topology. A new library may link sub-regions in the face to topologies, which will enable studies to explore the best fitting face topology that contributes to achieving higher accuracy.

This study attempted to derive quantitative evidence that discovers a sub-region in one's face based on that we perceive his or her facial skin color. We adopted domain-specific knowledge and data-driven techniques to answer the research question. With heuristic observations and experts' insight, the findings can be more elaborated and advanced to be practically more meaningful. It is expected that the method and findings of this study may motivate related investigation to obtain a better understanding of the human color perception that considers concerns and interests across diverse disciplines and industries.

5. CONCLUSION

In this study, we explored the skin color representative regions using the Humanae project's facial images. An individual image has a particular solid background color that the photographer has deliberately chosen to represent one's facial skin. Regarding a total of 2231 facial images, we applied the EOS, a 3D Morphable Face Model fitting library, and detected 3448 facial landmarks in each of 1052 women's faces. Also, having adopted the aesthetic units, we re-defined the 27 sub-regions to cluster the landmarks. Based on the L^*, a^*, and b^* values of the landmark vertices in each sub-region, we derived the color of the sub-regions. Finally, we estimated the color difference, ΔE, between sub-regions and background, and discovered that sub-regions of below lips and central cheeks appeared closest to the background. The sub-regions corresponded to the low Labial and upper Buccal of the aesthetic facial units. Furthermore, we found out that the tendency was consistent across four major ethnicities, including "White," "Latino Hispanic," "Black," and "Asian" groups as distinguished by the DeepFace.

REFERENCES

[1] Y. Zhu, M. R. Luo, S. Fischer, P. Bodrogi, and T. Q. Khanh, "Long-term memory color investigation: culture effect and experimental setting factors," J. Opt. Soc. Am. A **34**, 1757–1768 (2017).

[2] S. Bianco and R. Schettini, "Color constancy using faces," *2012 IEEE Conf. on Computer Vision and Pattern Recognition* (IEEE, Piscataway, NJ, 2012).

[3] S. Xie and J. Pan, "Hand detection using robust color correction and Gaussian mixture model," *Proc. IS&T/SID CIC19: Nineteenth Color and Imaging Conf.* (IS&T, Springfield, VA, 2011).

[4] Y. Yan and H.-J. Suk, "Affective effect of multi-source portraits under various illuminants on one scene," J. Imaging Sci. Technol. **64**, 20509-1–20509-9 (2020).

[5] I. S. Yun, W. J. Lee, D. K. Rah, Y. O. Kim, and B. y. Y. Park, "Skin color analysis using a spectrophotometer in Asians," Skin Res. Technol. **16**, 311–315 (2010).

[6] K. Kikuchi, Y. Mizokami, M. Egawa, and H. Yaguchi, "Development of an image evaluation method for skin color distribution in facial images and its application: Aging effects and seasonal changes of facial color distribution," Color Res. Appl. **45**, 290–302 (2020).

[7] H. Zeng and M. Luo, "Skin color modeling of digital photographic images," J. Imaging Sci. Technol. **55**, 30201-1–30201-12 (2011).

[8] H. Zeng and R. Luo, "Colour and tolerance of preferred skin colours on digital photographic images," Color Res. Appl. **38**, 30–45 (2013).

[9] J. D. Rigal, I. D. Mazis, S. Diridollou, B. Querleux, G. Yang, F. Leroy, and V. H. Barbosa, "The effect of age on skin color and color heterogeneity in four ethnic groups," Skin Res. Technol. **16**, 168–178 (2010).

[10] K. Xiao, J. M. Yates, F. Zardawi, S. Sueeprasan, N. Liao, L. Gill, C. Li, and S. Wuerger, "Characterising the variations in ethnic skin colours: a new calibrated data base for human skin," Skin Res. Technol. **23**, 21–29 (2017).

[11] Y. Wu, F. Yi, M. Akimoto, T. Tanaka, H. Meng, and Y. Dong, "Objective measurement and comparison of human facial skin color in East Asian females," Skin Res. Technol. **26**, 584–590 (2020).

[12] H. Yoshikawa, K. Kikuchi, H. Yaguchi, Y. Mizokami, and S. Takata, "Effect of chromatic components on facial skin whiteness," Color Res. Appl. **37**, 281–291 (2012).

[13] K. Kikuchi, C. Katagiri, H. Yoshikawa, Y. Mizokami, and H. Yaguchi, "Long-term changes in Japanese women's facial skin color," Color Res. Appl. **43**, 119–129 (2018).

[14] S. W. Hsiao, C. H. Yen, and C. H. Lee, "An intelligent skin-color capture method based on fuzzy C-means with applications," Color Res. Appl. **42**, 775–787 (2017).

[15] H. Choi, K. Choi, and H.-J. Suk, "Skin-representative region in a face for finding real skin color," Electron. Imaging **2017**, 66–69 (2017).

[16] A. Hernandez-Matamoros, H. Fujita, M. Nakano-Miyatake, H. Pérez-Meana, and E. E. Hernández, "A scheme to classify skin through geographic distribution of tonalities using fuzzy based classification approach," presented at the SoMeT, (2019).

[17] Y. Taigman, M. Yang, M. A. Ranzato, and L. Wolf, "Deepface: Closing the gap to human-level performance in face verification," *Proc. IEEE Conf. on Computer Vision and Pattern Recognition* (IEEE, Piscataway, NJ, 2014).

[18] A. Rosebrock, *Deep Learning for Computer Vision with Python: Starter Bundle* (PyImageSearch, Philadelphia, PA, United States, 2017).

[19] P. Huber, G. Hu, R. Tena, P. Mortazavian, P. Koppen, W. J. Christmas, M. Ratsch, and J. Kittler, "A multiresolution 3d morphable face model and fitting framework," *Proc. IS&T CIC24: Twenty-Fourth Color and Imaging Conf.* (IS&T, Springfield, VA, 2016).

[20] D. Poux, B. Allaert, J. Mennesson, N. Ihaddadene, L. M. Bilasco, and C. Dieraba, "Mastering occlusions by using intelligent facial frameworks based on the propagation of movement," *2018 Int'l. Conf. on Content-Based Multimedia Indexing (CBMI)* (IEEE, Piscataway, NJ, 2018).

[21] J. H. Choi, Y. J. Kim, H. Kim, S. H. Nam, and Y. W. Choi, "Distribution of Basal cell carcinoma and squamous cell carcinoma by facial esthetic unit," Archives of Plastic Surgery **40**, 387 (2013).

[22] M. Gonzalez-Ulloa, A. Castillo, E. Stevens, G. A. Fuertes, F. Leonelli, and F. Ubaldo, "Preliminary study of the total restoration of the facial skin," Plastic Reconstructive Surgery **13**, 151–161 (1954).